DOI: 10.18721/JPM.13415

AN OUTPUT POWER LEVEL OF THE FIBER-OPTIC INTERFEROMETRIC SCHEMES WITH FIBER BRAGG GRATINGS FOR MULTIPLEXING THE SENSITIVE ELEMENTS

L.B. Liokumovich[1], *A.O. Kostromitin*[2,1]

Ph.V. Skliarov[2,1], *O.I. Kotov*[1]

[1] Peter the Great St. Petersburg Polytechnic University, St. Petersburg, Russian Federation;

[2] Concern CSRI "Elektropribor", St. Petersburg, Russian Federation

The paper continues a series of articles devoted to the procedure proposed by the authors how to calculate the required elements' parameters and the output optical power level of the fiber-optic interferometric schemes with time-division multiplexing (TDM) of sensing elements. In particular, the schemes based on fiber Bragg gratings have been analyzed. The proposed method enables to ensure uniformity of powers of optical signals from individual sensing elements, as well as to evaluate how the deviations of elements' parameters from the nominal ones influence the optical powers. According to the calculation methodology, a sequence of applying the required expressions was substantiated and some obtained results and an analysis of characteristic behaviors for the considered optical fiber circuits were exemplified. The proposed approach was recommended for design of interferometric optical fiber sensors with multiplexed sensing elements.

Keywords: fiber-optic interferometric sensor, Bragg grating, optical power, time-division multiplexing

Citation: Liokumovich L.B., Kostromitin A.O., Skliarov Ph.V., Kotov O.I., An output power level of the fiber-optic interferometric schemes with fiber Bragg gratings for multiplexing the sensitive elements, St. Petersburg Polytechnical State University Journal. Physics and Mathematics. 13 (4) (2020) 135–147. DOI: 10.18721/JPM.13415

Introduction

Fiber optic measurement systems and devices have a number of advantages, associated primarily with the possibility of using fully optical electroneutral and passive fiber-optic sensing circuits, as well as circuits for coupling the sensing elements to the optoelectronic part [1]. Interferometric systems are an attractive option of fiber optic measurement systems [2], due to the fact that they offer the best resolution. In recent decades, such measurement systems have been actively developed and implemented in various fields, for example, in navigation systems, in hydroacoustics, in the oil and gas industry, in measuring equipment for medical purposes [3–6].

Practical implementations of such measurement systems mainly involve multiplexing of a set of fiber optic sensing elements (SE) in a single path connected to the optical source and the photodetector. The principle of Time Division Multiplexing (TDM) is most commonly used for this purpose [6]: instead of continuous light radiation, optical pulses are fed into a fiber optical circuit, and a sequence of output pulses is generated at the output of the circuit in response to each input pulse carrying information about the corresponding SE and the impact on it. The structure of such an optical circuit and the parameters of all elements (sensitive fiber sections, beam splitting elements, reflectors, etc.) must correspond to a whole range of relations in order to ensure the operability of such a measurement system and its efficiency.

An important component in the set of parameters for fiber-optic circuits with multiplexing SE in the interferometric measurement system is the so-called energy efficiency, namely, the level of power of the

output pulses relative to the pulse power at the input of the circuit. The energy efficiency directly affects the achieved signal-to-noise ratio in the generated series of interference signals and, consequently, the level of output noise in the measuring system. Nevertheless, the available literature does not present comprehensive methods for calculating the energy efficiency of such fiber-optic circuits. Only simplified estimates are typically given for particular cases, when it is impossible to take into account important factors (losses of optical power in the elements, possible deviations of actual parameters from the required optimal values, including random deviations) [7]. The approximations used often perform poorly in practice, for example, too large or even an infinite number of multiplexed SEs is assumed [7], while up to 16 or 32 SEs are generally multiplexed in real systems, and circuits with eight or even four SEs are frequently constructed.

An example of a consistent method of energy calculation for fiber optic circuits with multiplexed SEs is given in our earlier study [8], which also discusses the possibilities of analyzing the characteristics of the given circuits based on the developed calculation method.

In this paper, we propose a similar consideration of the energy calculation procedure and a brief analysis of the results obtained for a circuit of another type, where fiber Bragg gratings (FBG) are used as light-splitting elements [10]. This option is attractive for practical applications, in particular because it yields improved energy characteristics.

However, such gratings have a serious drawback: they lead to a crosstalk between signals from different SEs [10].

In view of the above, it seems extremely important to produce a well-founded comprehensive calculation of the optimal system of FBG parameters and the power level of the output optical radiation in such circuits taking into account all key element parameters, as well as parameters that characterize the level of parasitic crosstalk.

Circuit under consideration and principles of calculations

The subject of the analysis is an optical fiber path for a multiplexed interferometric measuring system. Its sensing elements are fiber sections mounted in certain structural units; the latter are optimized to convert the target perturbation passing through this section into a change in the phase delay of light. A key part of such a system is an optical circuit where N fiber SEs are combined into a certain path using splitters and reflectors [11].

In reflection-type circuits, the same fiber output and input can actually be used as the input and output of the radiation (an additional Y-splitter or circulator can be used in the instrumentation unit of the system for separation). In feed-through circuits, the input and output are at different ends of the path with the SE. If a short optical pulse of power P_{in} is fed to the circuit input, then a sequence of output pulses of power p_n should be generated at the circuit output, where the nth pulse goes through the SEs from the first to the nth and does not go through other SEs. Typically, $N + 1$ pulses with numbers from 0 to N are generated, where the pulse with the number zero ($n = 0$) does not pass through any SEs. These pulses will be delayed relative to each other due to the delay in passing the corresponding system of links in the SE circuit.

For the circuits considered in our previous study [8], as well as those considered in this paper (including the circuits given in Appendix 1), the light delay in passing the circuit links is primarily determined by the delay in propagation through fiber SEs. Next, because the so-called compensation interferometer is used in the interrogation unit, the pulses are separated, shifted, and each initial pulse is combined with the previous one. As a result, due to separate processing of pulses, the result of interference of pulses whose phase difference is given by the phase delay of light in the nth SE can be recorded at the output of the compensated interferometer, and, therefore, the data about the target impact on this element can be collected. The input pulses are repeated during operation of the measuring system, with a sequence of interference signal samples from each SE (from each channel) produced as a result.

The analysis of such circuits implies different types of description and calculations associated with different types of factors, which should be considered and coordinated to maintain acceptable performance of the system and optimize its characteristics. Here we consider the energy efficiency factor of the circuit, i.e., analyze the optical power levels of the pulses generated by the circuit.

By analogy with the approach used and described in [8], this work implies the choice of parameters of dividing and reflecting elements that ensure the same power of all pulses

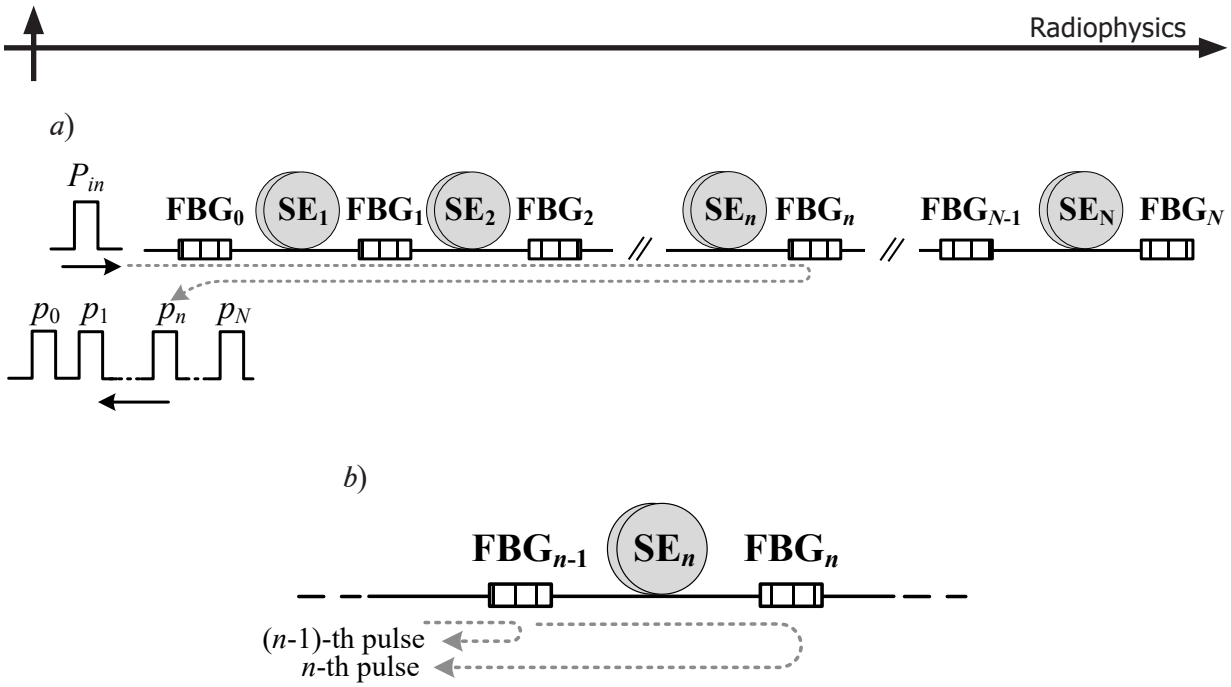

Fig. 1. Example of a circuit based on FBG with N sensing elements (*a*), *nth* link of this circuit (*b*); Sensitive Element SE*i*; Fiber Bragg Grating FBG*i*; P_{in}, p_n are the input and output pulse powers, respectively

generated by the circuit: $p_n = P_0$. In this case, the main parameter that characterizes the energy efficiency of the optical circuit is the relative level of the optical power of the generated series of pulses $P_{norm} = P_0/P_{in}$.

The types of fiber optic circuits with multiplexing SEs analyzed in [8] are arranged so that the nth reverse pulse reflected from the nth SE is split twice by the splitter and, consequently, the P_{norm} value decreases rapidly with increasing N (at best, the relation is expressed approximately as $1/N^2$).

Let us also consider another configuration of circuits with multiplexing of fiber SEs, more advantageous from the standpoint of the P_{norm} level. An example is a circuit attractive for practical use (Fig. 1), with partially reflecting fiber elements (semi-transparent mirrors). Fiber Bragg gratings (FBG) are primarily used as the latter. Compared with the circuits described in [8], the configuration that includes FBG has a different form (see Appendix 1), which has two important features (positive and negative):

on the one hand, the circuit generates a significantly higher relative power level of pulses P_{norm}, which decreases rather slowly with increasing value of N;

on the other hand, in addition to the main sequence of output pulses, additional parasitic pulses are generated in the circuit, which cause crosstalk between the target signals from different SEs.

As shown in Appendix 1, not only circuits with feed-through reflectors but also with splitters can have such properties, and they can serve as a basis for implementing circuits of both reflective and feed-through types. The presence of significant crosstalk makes practical applications of the described variants considerably less attractive, effectively eliminating the benefits of such schemes in terms of energy efficiency. To reduce the level of crosstalk, it is necessary to choose the parameters so that the relative level of power P_{norm} decreases. All of this makes it the more important to develop adequate methods for calculating such circuits.

The general principle and basic stages of calculating the parameters of the elements (in this case, these are primarily the reflectivities of the FBG) and the power of the output optical pulses are completely similar to the approach described in [8]. Part of the calculation procedure is related to obtaining and using multiplicative expressions to calculate p_n, assuming that all circuit element parameters are given. The other part of the procedure implies the derivation of recurrence relations for the main elements of the nth circuit, making it possible to fulfill the condition that the powers of all output pulses be equal ($p_n = P_0$). These parts of the calculation expressions allow not only to determine the required values of circuit element parameters but also to take into account

and analyze the influence of various factors, such as losses in elements (including random ones), deviations of actual element parameters from nominal or prescribed values, and other factors inevitably present in real-life design of circuits.

Procedure for calculating the parameters of FBG and general analysis of power level of output pulses

To describe the operating principles of an FBG as a reflecting element, we will use the reflectivity R, equal to the ratio of power of the optical radiation entering the FBG to that of the radiation directed back by the grating. The power of the radiation that has passed through the FBG is described by the transmittance K at the generation wavelength, which is given by the expression

$$K = (1 - R)(1 - \alpha_{el}),$$

where the first factor accounts for the fact that part of the power is directed backwards by the grating, and the second factor accounts for the presence of internal (excessive) optical power losses; these losses are characterized by a small parameter α_{el}.

We also use the power transfer coefficient K_f for a section of fiber with an SE, taking into account the optical power loss in this section. Since the fiber in the sensitive elements can be twisted into a coil or otherwise assembled into the SE structure, the magnitude of these losses can be significant, even despite the relatively small length of this fiber optic section. If there are spliced or detachable connections in the circuit, losses in them should also be taken into account in the values of the coefficients K_f.

In practice, it is convenient to characterize losses in decibels, using standard ratios

$$\alpha_{el[\mathrm{dB}]} = 10 \cdot \lg(1 - \alpha_{el}),$$

$$a_f = 10 \cdot \lg K_f.$$

The values of K_f and α can be found from a_f and $\alpha_{el[\mathrm{dB}]}$ based on trivial inverse relations.

Given the parameters and notations introduced, if we consider the passage of the input pulse to the nth FBG and back (see Fig. 1, *a*), it is easy to formulate the multiplicative expression for p_n:

$$p_n = P_{in} \cdot R_n \cdot \prod_{q=1}^{n} \left(K_{q-1}^2 \cdot K_{fq}^2 \right). \qquad (1)$$

Eq. (1) implies that if the upper limit of the product is less than the lower limit (which is the case when $n = 0$), then the product is equal to unity. In practice, we can often assume that all SEs are equivalent and K_f does not depend on the value of n. Then this parameter can be excluded from the product in expression (1) and an additional factor K_f^{2n} can be used.

Analyzing one link in the circuit and comparing the path difference of the $(n - 1)$th and the nth pulse (see Fig. 1, *b*), we can obtain the equation corresponding to the balance $p_{n-1} = p_n$; it has the following form:

$$R_{(n-1)} = K_{n-1}^2 \cdot K_{fn}^2 \cdot R_n = \left(1 - \alpha_{el(n-1)}\right)^2 \left(1 - R_{n-1}\right)^2 K_{fn}^2 \cdot R_n, \qquad (2)$$

where n can vary from 1 to N.

Ratio (2) is a quadratic equation with respect to $R_{(n-1)}$, which has a solution in the form

$$R_{(n-1)} = \frac{a + 1 - \sqrt{2a + 1}}{a}, \qquad (3)$$

where the notation $a = 2[(1 - \alpha_{el\,(n-1)}) K_{fn}]^2 R_n$ is used.

The second solution of Eq. (2) has a similar structure, but with a plus sign before the square root, and does not correspond to the physical sense in the given situation, because it leads to obtaining a value $R > 1$.

The recurrence relation (3) can be applied if two conditions are fulfilled.

First, it is necessary to give some value for the reflectivity of the closing mirror R_N, relative to which we can then calculate the reflectivities of other FBGs. The choice of this value and its influence will be discussed below.

Second, relation (3) includes the parameters K_{fn} (for $n = 1, 2, \ldots, N$) and α_{eln} (for $n = 1, 2, \ldots, N - 1$) related to the optical power loss in the circuit elements. The transfer coefficients K_{fn} depend on the level of losses in the SE, and they are not related to the choice of FBG, but must be known. However, the internal losses α_{el} in the FBG can be generally related to the value of R of the grating, and this relationship may be different depending on the technologies by which the grating was fabricated and installed in the optical circuit.

For a rigorous formal solution of the given problem, the dependence of α_{el} on R must be given in some form, Eq. (2) must be solved relative to R_{n-1} with this dependence taken into account, and the result may differ significantly from the one given by Eq. (3).

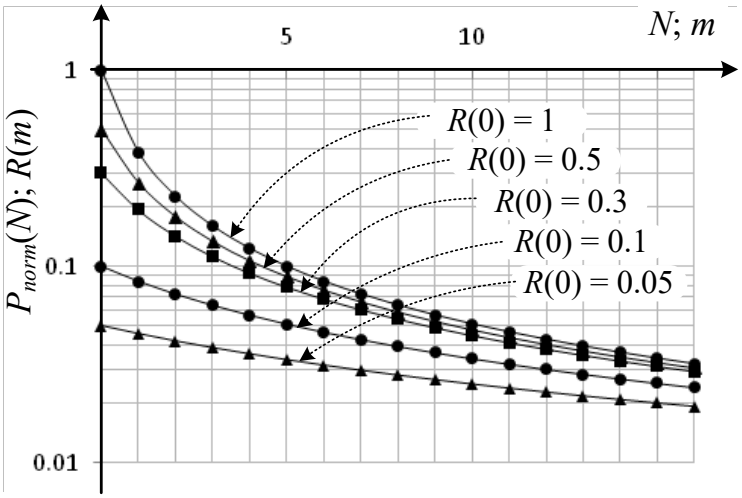

Fig. 2. Dependences of relative pulse power P_{norm} on the number of elements N (N varies from 1 to 16) and reflectivity R on the lattice number m (numbering from the end of the path, n is the circuit link number, $m = N - n$ and also varies from 0 to 16) for different reflectivities $R(0)$ of the final element

In view of the above, it is problematic to obtain a specific solution of Eq. (2) for the general case of the $\alpha_{el}(R)$ dependence. Therefore, it is proposed to specifically use relation (3) in the calculations, with some fixed value independent of n serving as α_{eln} (a typical or average value for the FBG intended to be used). In this case, if the condition of small losses $\alpha_{eln} << 1$ is fulfilled rigorously enough, then the influence of the difference of α_{el} due to the difference of R_n will have little effect on the obtained values of p_n. Moreover, after the reflectivities R_n of the gratings are calculated, the data on the actual losses in the FBGs with these reflectivities can be subsequently taken into account when analyzing the influence of this factor on the p_n values.

If we take $\alpha_{eln} = \alpha_{el}$, the recurrence relation (3) can be written in a simpler form taking into account the above explanations:

$$R_{(n-1)} = \frac{K_{fn}^2 \cdot R_n + b - \sqrt{K_{fn}^2 \cdot R_n + b^2}}{K_{fn}^2 \cdot R_n}, \quad (4)$$

introducing a constant $b = 0.5/(1 - \alpha_{el})$.

Choosing some level of reflectivity of the last reflector R_N, we can further obtain values for other reflectivities Rn from $n = N - 1$ to $n = 0$ by recurrence expression (4) in turn.

After the set of required grating reflectivities Rn is determined, the final stage of calculations involves finding the pulse powers p_n based on expression (1). If the parameters K_{fn} and α_{eln} do not depend on n, then, according to the principle by which expression (4) is derived, all p_n will be the same and equal to P_0. Therefore, to estimate P_0, we can use, for example, the simplest relation

$$P_0 = p_0 = P_{in} \cdot R_0.$$

On the other hand, if there is a priori information about the actual values of K_{fn} and α_{eln}, p_n can be found by expression (1) to consider their mean and standard deviations from P_0. If there is data on the relation between the excess losses in the FBG and the grating reflectance, α_{eln} values can be found from the calculated R_n to account for the n-dependent losses when calculating p_n based on expression (1).

In addition, for various reasons, the values of R'_n (the real reflectivities of the FBGs that are intended to be used) may differ from the values of R_n (initially calculated). If such data are available, they can be taken into account at this stage by using R'_n rather than R_n in expression (1). An example is the case, when the reflectivities R'_n of real FBGs are set with rounding to some level, then the calculated R_n values should be rounded; another case is when the calculations are performed to study the influence of random deviations of parameters of real elements from the preset ones.

For general analysis of the energy efficiency of circuits, it is usually sufficient to determine the relative level P_{norm}; to calculate this parameter, substitute $P_{in} = 1$ in Eq. (1).

To illustrate the form of general dependences, we will give examples of calculations

for the case when losses are neglected, assuming that $K_{fn} = K_n = 1$. For this purpose, Fig. 2 shows the result of the calculation of R_n when $n = 0, 1, ..., 16$, when $R_N = 100\%$, 50%, 30%, 10% and 5%. To simplify further analysis, the dependences $R(m)$ are given, where m is the number of the FBG from the end of the path, i.e., $m = N - n$. Given this numbering, $R_N = R(0)$. According to the principle of recurrence calculation, the presented dependences reflect the result for any number of sensitive elements N in the range from 0 to 15. For a given N, we should use the first $N + 1$ values of the coefficients $R(m)$, where m takes values from 0 to N. The remaining calculation coefficients with values $m > N$ are not needed in this case.

As already mentioned, if we do not introduce the differences between the actual values of reflectivities and the initial calculated ones into the power calculations by formula (1), the power P_0 can be estimated as $P_0 = P_{in} \cdot R_0$. Then

$$P_{norm} = R_0 = R(m)|_{m=N}.$$

It follows that the presented $R(m)$ dependences simultaneously characterize the relationship between the values of P_{norm} and N, which is also evident from Fig. 2. To analyze the specific values of $R(m)$ or $P_{norm}(N)$ shown in Fig. 2, these values are given as a table in Appendix 3.

If $R_N = 1$ (it corresponds to $R(0) = 1$ in Fig. 2), the dependence $P_{norm}(N)$ is proportional to $1/N$ with good accuracy; approximation gives the dependence $P_{norm} = 0.45 / N^{0.95}$ for the values of N from 1 to 15. The dependences for the reflectances of 50%, 30% and 10% ($R(0) = 0.5$, 0.3 and 0.1) are also in good agreement with the power dependences, but the exponent decreases, and the dependency at $R_N = 10\%$ is already proportional to $1/\sqrt{N}$. The dependence at $R(0) = 0.05$ ($R_N = 5\%$) is better described by a logarithmic rather than a power dependence; the approximation gives the function

$$P_{norm} = 0.051 - 0.011 \cdot \ln N.$$

If we compare these results with similar calculated data for circuits based on splitters, which are free of channel crosstalk [9], a significant gain in the level of output optical pulses is evident for all values of N, even if relatively low values of R_N, such as 5%, are used. Moreover, in the case of an alternative type of circuit, the $P_{norm}(N)$ dependences can be approximated by power dependences, with exponents close to 2 or higher [8].

Obviously, for any value of N, the maximum level of P_{norm} is provided at $R_N = 1$. However, reducing the reflectivity of the final FBG and, accordingly, of the other gratings allows to reduce the level of channel crosstalk. A quantitative characteristic of this coupling is the coefficient K_{cr} (see Appendix 2). If losses in the fiber elements are neglected, then this coefficient is introduced by expression (a4) for the given circuit and has the form

$$K_{cr} = R^2_{N-1} R_{N-2} / [R_N (1 - R_{N-1})^2].$$

Given the numbering $R(m)$ used in Fig. 2, we can write

$$K_{cr} = R(1)^2 \cdot R(2) / [R(0)\,(1 - R(1)^2].$$

Taking into account the data obtained (see, for example, Appendix 3), the crosstalk coefficients K_{cr} for the cases $R_N = 100\%$, 10% and 5% take values of 0.087; $6.06 \cdot 10^{-3}$ and $1.91 \cdot 10^{-3}$, respectively.

Thus, a 20-fold decrease in the reflectivity R_N of the final reflector leads to a 45-fold decrease in the crosstalk coefficient K_{cr}. However, the relative power level P_{norm} of optical pulses formed by the circuit will decrease. This is demonstrated

Table 1

Dependence of optical power level of generated pulse system on the values of main circuit parameters

R_N	K_{cr}	P_{norm}		
		$N = 4$	$N = 8$	$N = 16$
1.00	0.087	0.123	0.063	0.032
0.10	6.06·10–3	0.056	0.039	0.024
0.05	1.91·10–3	0.036	0.028	0.019

Notations: N is the number of sensitive elements, R_N is the reflectivity of the last reflector, K_{cr} is the crosstalk coefficient.

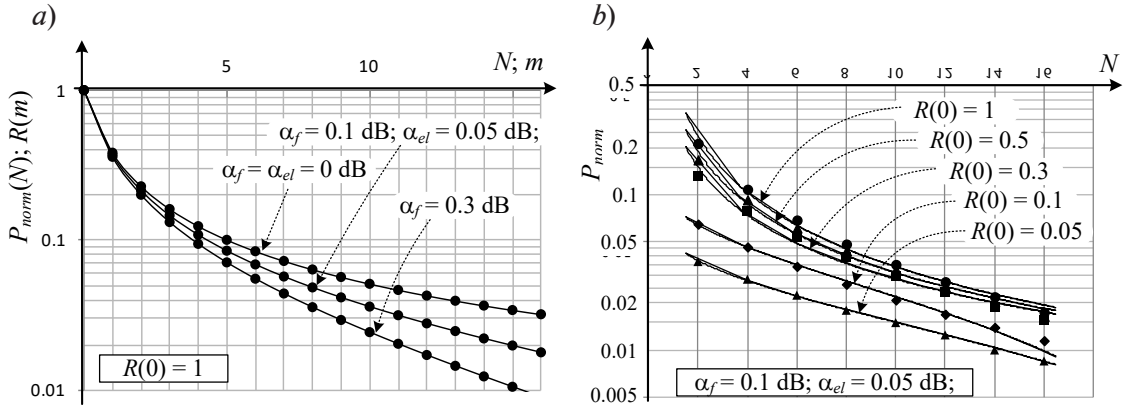

Fig. 3. Examples of calculations accounting for optical power losses in the circuit elements. The $R(m)$ dependences (or $P_{norm}(N)$, the dependences coincide) are given for $R(0) = 1$ and different values of loss factors (*a*) and $P_{norm}(N)$ for different values of R_N (*b*)

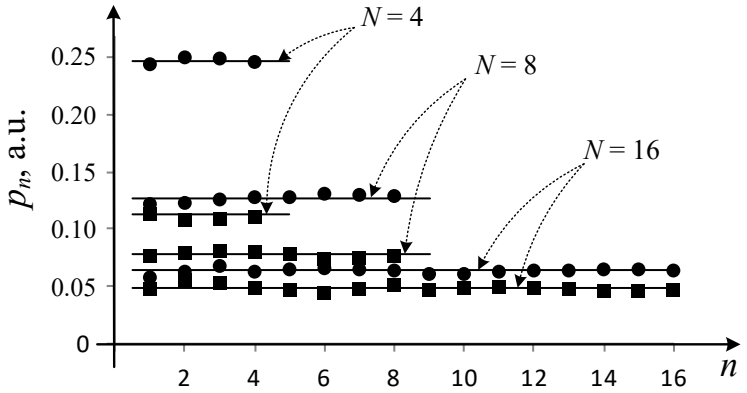

Fig. 4. Dependences of output pulse power on circuit link number for different N and two R_N values, %: 99 and 10 (circles and squares, respectively). The values of p_n are normalized to the input pulse power $_{Pin}$. We consider the case when R'_n values are obtained with R_n rounded to 1%; solid lines correspond to P_{norm} levels with no rounding.

in Table 1, where the values of R_N, K_{cr}, and P_{norm} are compared. At the same time, according to Table 1, a decrease in crosstalk by almost two orders of magnitude is achieved with a relatively small decrease in P_{norm}. The power level is reduced by 3.4 times for a circuit with four SEs. For more attractive configurations with $N = 8$ and $N = 16$, the power decreases less dramatically: the P_{norm} value decreases by 2.3 times for eight SEs, and by only 1.6 times for sixteen.

Effect of power loss in circuit elements and differences between calculated and actual reflectivities

The given calculation procedure allows to account for the losses in the circuit elements. Comprehensive analysis of the influence of losses on the $R(m)$ and $P_{norm}(N)$ dependences is somewhat complicated due to too high variability of possible parameter values with their significant influence on the circuit characteristics. Therefore, we will confine ourselves to examples of calculations accounting for such losses and their influence. For example, Fig. 3,*a* shows the $R(m)$ or $P_{norm}(N)$ dependences (with the numbering introduced, these dependences will coincide, see explanations above). The graph demonstrates the reduction in the reflectivities of the FBG required to equal the power of the output pulses, as well as the reduction in the relative level of this power due to accounting for the losses in the fiber optic SE and the excess losses in the FBG. In this example, the element losses of all circuit links are assumed

Table 2

Effect of rounding the calculated R_n values to 1% for calculations of optical power of the output pulses using Eq. (1)

N	R_N,%	P_{norm} (no rounding)	${}^{mean}p_n$	$({}^{SD}p_n / {}^{mean}p_n)$, %
4	99	0.246	0.247	1.1
	10	0.113	0.11	2.0
8	99	0.1267	0.1266	2.5
	10	0.0783	0.0776	3.0
16	99	0.006357	0.006369	6.0
	10	0.004842	0.004863	3.6

Notations: P_{norm} is the relative level of output power with no rounding; ${}^{mean}p_n$ is the mean value of p_n, ${}^{SD}p_n$ is the standard deviation *of* p_n, normalized to the input pulse power $_{Pin}$; other notations are identical to those given in Table 1.

to be the same. Apparently, accounting for insignificant losses has a noticeable effect on the calculated dependences, especially when the number of SEs is large.

Fig. 3, *b* show the results of calculation of $P_{norm}(N)$ at different values of $R_N = R(0)$ for the case of losses expressed in terms of $a_f = 0.10$ dB и $\alpha_{el} = 0.05$ dB. In spite of noticeable influence of losses on the dependences shown (if they are compared with the curves in Fig. 2), the general conclusion about a relatively small decrease in the output power level with a significant decrease in the values of R_N and K_{cr} remains valid.

As already noted, an important advantage of the given procedure is that it allows to account for the differences between the calculated and actual parameter values of the circuit elements, as well as to analyze the impact of such differences.

As an example, consider the case where reflection coefficients for real FBGs can be given with a finite accuracy, for example, 1%. Appendix 3 shows the result of such rounding of values of R_n obtained neglecting losses. Referring to the data in the table in Appendix 3, we can see that rounding can make significant differences between R'_n and R_n, since the initial values of R_n themselves are small, especially with relatively large values of N and small reflectivities R_N. The effect of rounding on the irregularity of p_n is illustrated by the graphs in Fig. 4, where, as an example, the calculated values of p_n values are given with rounded coefficients R'_n substituted into Eq. (1). It can be seen that the variations of p_n introduced are noticeable but not significant. More accurate quantitative data characterizing the dependences shown in Fig. 4 are given in Table 2. We can also see that the deviation of the mean pulse powers differs from the initial estimate of P_{norm} only in the third significant digit. Even for $N = 16$, where the influence is more significant due to the low initial values *of* R_n, the standard deviation of the set of p_n values is 6 %, which can be deemed acceptable.

Similarly, it is possible to consider other cases of deviations of actual parameters from the calculated ones when calculating initial values of R_n (including actual values of losses in elements) and to analyze their influence on the obtained values of p_n. In this case it is possible to account for and analyze both regular and random deviations of parameter values.

Similarly, other factors of deviation of R'_n from R_n can be taken into account. The last stage of calculations by Eq. (1) can also involve accounting for the differences of actual values of other parameters and the values used in the first stage of calculations, calculating the initial values of R_n, and analyze their influence on the obtained values of p_n. Both regular and random deviations of parameter values can be taken into account and analyzed.

Conclusion

We have proposed an ideology for calculating the parameters of the elements of interferometric fiber optic schemes of multiplexed fiber optic sensors using FBG, which makes it possible to optimize the circuit to achieve the maximum level and visibility of the generated interference signals. The procedure for obtaining expressions to calculate the reflectivities of FBGs that provide the same output pulse power is described. The proposed calculation procedure accounts for the optical power losses both in the FBG and in the fiber sections of the sensing

elements. It is established that the calculations can account for the influence of differences between the parameters of the elements used and obtained in the initial calculation and the actual parameters of the elements that will be used for creating a real optical circuit.

We have provided examples of calculating the FBG parameters in the given circuit for different numbers of sensitive elements and different levels of crosstalk in the circuit. The examples confirm that it is possible to analyze the effect of losses in the circuit elements and use rounded values of the FBG reflectivities.

The presented methods and calculation results can be directly used to design fiber optic interferometric measurement systems based on multiplexing of sensing elements in a circuit with FBG.

Appendix 1

Two classes of fiber optic circuits with multiplexed sensitive elements

To explain the peculiarities of the analyzed circuit, let us briefly describe two classes of fiber optic circuits for interferometric systems with multiplexing of sensing elements (SEs). Characteristic examples of circuits of the first class include the ones considered in [8] and shown in Fig. A1. The first one is a reflective circuit, the second one is a feed-through type.

Another class of optical circuits is possible; examples are shown in Fig. A2. This class also includes reflective (*a*, *b*) and feed-through (*c*) circuits. In such circuits, low-loss reflective fiber elements, such as FBGs, can be used in partial reflection/transmission mode.

In all these circuits, the *n*th output optical pulse is formed by passing through the sensing elements from the 1st to the *n*th. In reflective circuits with combined input/output fiber output, the pulse passes through these SEs twice; in circuits with separated input and output fibers, the pulse passes through the SEs once.

Evidently, for circuits in Fig. A1, the *n*th pulse that passes through each SE from the first to the *n*th also passes through the *n*th splitter of this circuit along the forward path (where the larger share of power is transmitted) and passes twice through the splitter of the *n*th link along the crosstalk direction (where a smaller share of power is transmitted). The situation is similar in circuits in Fig. A2 (*b* and *c*), but the *n*th pulse passes through the *n*th splitter in the crosstalk direction only once. The same happens in the case of the FBG scheme (*a*), if we assume that the passage of light through the FBG corresponds to the forward path through the splitter, and the reflection from the grating corresponds to the crosstalk path through it. It is the additional crosstalk passage through the splitter in the circuits of the first class that leads to a significant reduction in the pulse power level, compared with the circuit of the second class, because the required crosstalk transmittance of the splitters is small and decreases with increasing number N of the SEs.

However, it is clear that the *n*th output pulse can also be formed by other propagation paths in circuits of the second class, which is described in more detail in Appendix 2. For example, in the circuit in Fig. A1,*b*, the pulse may not pass through the *n*th SE, but pass through any previous element twice. The pulse in the circuit

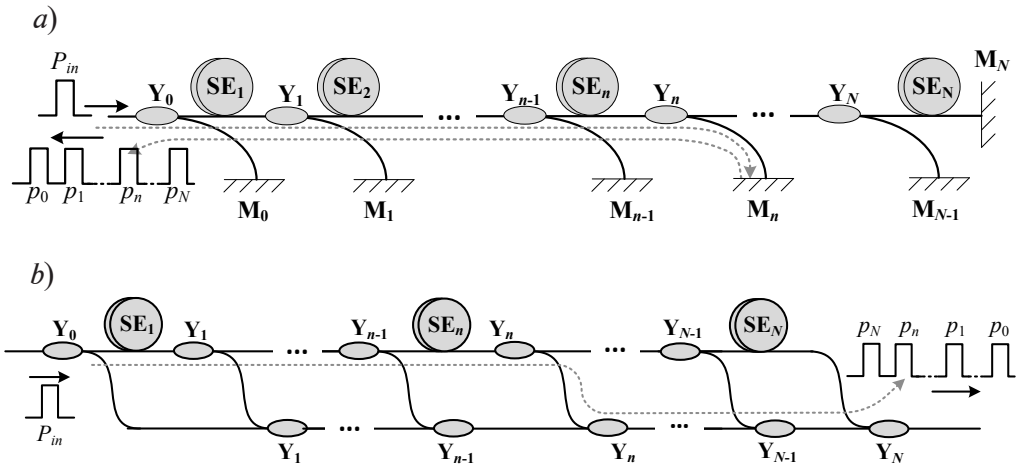

Fig. A1. Fiber optic multiplexing circuits of the first class: reflective type based on splitters and mirrors (*a*) and feed-through type based on splitters (*b*); Sensitive Element SE*i*; Y-type fiber splitter Y_i; mirror M_i; input and output pulse powers P_{in} and p_n, respectively

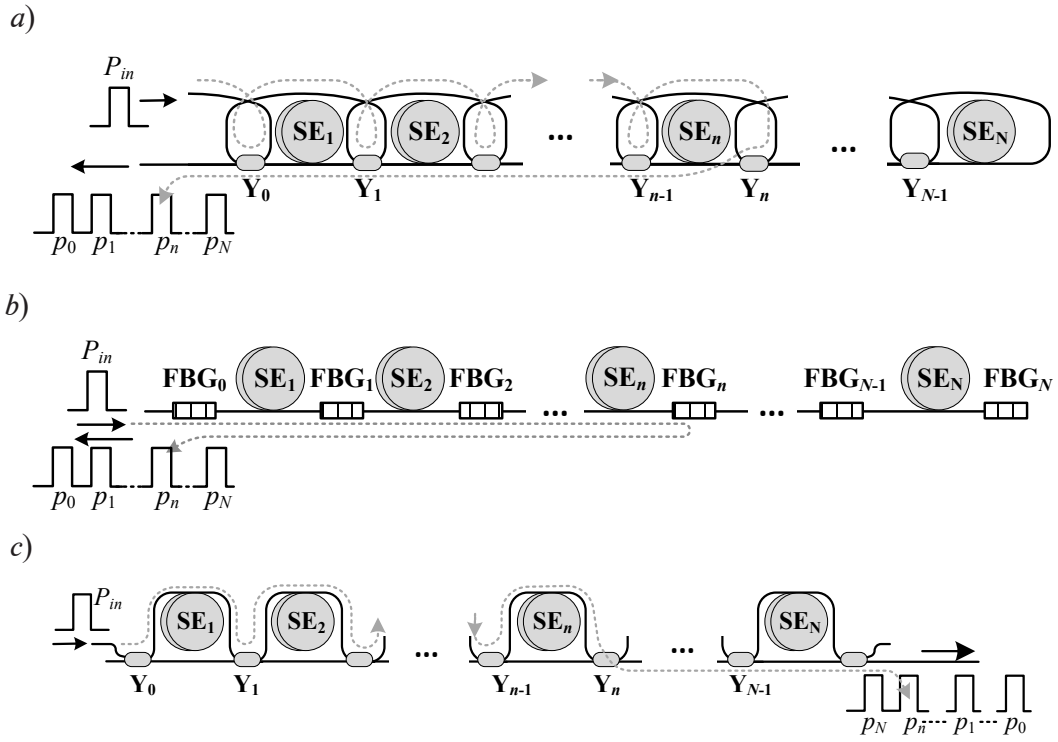

Fig. A2. Fiber optic multiplexing circuits of the second class: reflective based on FBG (*a*) and splitters (*b*); feed-through type with splitters (*c*);
FBG_i are Fiber Bragg Grating, other notations are identical to those in Fig. A1

in Fig. A1,*c* can pass the SEs from 1 through $(n-1)$, then pass by the *n*th SE, and then pass through any of the subsequent ones. If the total number of SEs passed is *n*, then this pulse will be in the *nth* position in the output sequence of pulses. As a result, pulses whose phases differ not only by the delay in the *n*th SE, but also by phase delays in other SEs subsequently participate in generating the interference signal of the *n*th channel. Generation of an additional *n*th pulse is connected with additional crosstalk passes of splitters and significant additional attenuation. Nevertheless, the presence of not only main but also additional pulses in the output sequence leads to cross-influence of the measured target perturbations in different channels. The generation of additional pulses in the FBG circuit is analyzed in more detail in Appendix 2.

Note that there are no alternative ways for forming the *n*th pulse in the output sequence in circuits of the first class (see, for example, Fig. A1). However, in order to exclude such a possibility in the configuration of the circuit, an additional crosstalk pass of the splitter is inevitably introduced, with the energy efficiency of the circuit considerably deteriorating.

Thus, reducing the relative power level of the output pulses can be regarded as payback of sorts for eliminating crosstalk of channels, and vice versa, it is possible to increase the pulse power level if crosstalk of channels is allowed.

Appendix 2

Generation of parasitic output pulses in the multiplexing circuit based on FBG

Let us consider the generation of additional output pulses, which determine the crosstalk of channels in the given fiber optic scheme with FBG. The main sequence of output pulses is formed when the *n*th pulse passes to the *n*th grating and back, and reflection occurs once (this path is denoted by number *1* in Fig. A3). However, other paths of the circuit, which have the same length, are also possible, due to which additional pulses coinciding with the main *n*th pulse are generated. First of all, such additional cases are associated with a single additional repeated reflection between the FBGs, where the reflection occurs three times, with the light reflected once from the $(n-1)$ th FBG. Such cases are denoted by numbers *2* to *4* in Fig. A3. Number *3* corresponds to

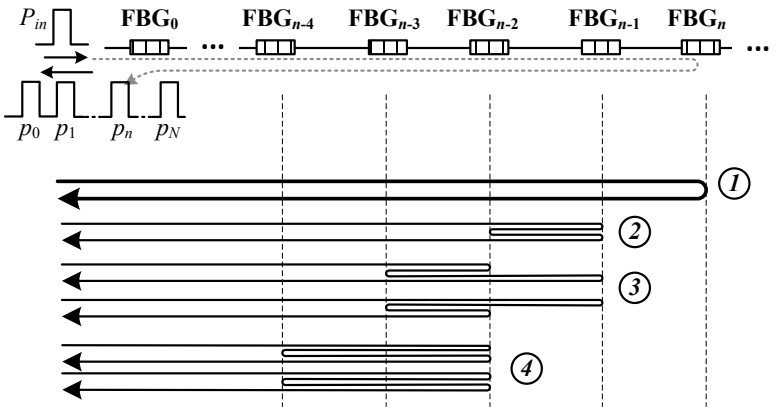

Fig. A3. Cases (*1* – *4*) of the light passing through the FBG circuit with additional *n*th pulse generated at the output

two cases with reflections from the FBG and numbers $(n-2)$ and $(n-3)$, which differ in the direction of the passage. Similar paths with repeated reflections between any two adjacent FBGs can be proposed. Importantly, in this case the additional pulse is attenuated and its power differs from the power of the main pulse by the multiplier

$$k_{crn}(k) = R_k R_{k-1} K_{fk} R_{n-1} \times \\ \times [R_n (1-R_{n-1})^2 (1-\alpha_{el(n-1)})^2 K_{fn}]^{-1}, \quad \text{(a1)}$$

assuming an additional repeated reflection from the FBG with the numbers k and $(k-1)$ (it is assumed that $k \le n$).

The first four multipliers take into account the attenuation factors of parasitic pulse added to the attenuation factors of the main pulse, and the multipliers in square brackets take into account the attenuation factors that the main pulse has but the parasitic pulse does not. Additional reflection can occur not only between neighboring FBGs, but also several positions apart (e.g., see Fig. A3, case *4*). In this more complex case, the attenuation coefficient has additional components:

$$k_{crn}(k, m) = R_k R_m (K_{fk} K_{f(k+1)} \dots K_{fm}) \times \\ \times \{R_{n-D} \cdot [R_n (1-R_{n-\Delta})^2 \times \\ \times (1-\alpha_{el(n-\Delta)})^2 K_{fn} \dots K_{f(n-\Delta)}]^{-1}\}, \quad \text{(a2)}$$

where $\Delta = k - m$; any different k and m $(k \ge m)$ less than n can be chosen.

Case *4* in Fig. A3 is the variant for $k = n-2$, $m = n-4$.

As follows from the explanations, the *n*th can travel by many additional trajectories. Although their number is finite for a particular value of N, it is difficult to comprehensively consider the general case. It seems appropriate to focus on the variant when the additional pulse has the maximum power. According to the procedure developed in this paper, equalizing the output pulse powers requires that the condition $R_n > R_{n-1}$ be satisfied. If we also assume that the losses in the elements are small and approximately equal, it is easy to see that the highest level of additional pulses with a single repeated reflection will be in case *2*, shown in Fig. A3 for $k = n$ and $n = N$. Therefore, taking into account expression (*a*1), we can introduce the following coefficient as some quantitative measure characterizing the relative level of power of additional pulses and crosstalk:

$$K_{cr} = k_{crN}(N-1) = R^2_{N-1} R_{N-2} K_{f(N-1)} \times \\ \times [R_N (1-R_{N-1})^2 (1-\alpha_{el(N-1)})^2 K_{fN}]^{-1}. \quad \text{(a3)}$$

The coefficient K_{cr} for the case where losses in circuit elements can be neglected can be written as

$$K_{cr} = k_{crN}(N-1) = R^2_{N-1} R_{N-2} K_{f(N-1)} \times \\ \times K_{cr} = R^2_{N-1} R_{N-2} / [R_N (1-R_{N-1})^2]. \quad \text{(a4)}$$

In addition to the trajectories shown in Fig. A3, the *n*th pulse can be generated by different means, due to double reflection. In this case, the pulse is reflected, for example, from the $(n-2)$th FBG and is re-reflected twice more between it and the $(n-3)$th FBG. However, it is evident that in this case the power level will have a significant additional attenuation, primarily due to additional multiplication by two FBG reflectances. Therefore, it is more logical to assume the coefficient (*a*3) to be the measure of crosstalk.

Appendix 3

Results of calculating the $R(m)$ dependences

The results of calculations of $R(m)$ dependences are shown graphically in Fig. 2 (m is the number of FBGs from the end of the circuit). However, for more accurate understanding and analysis of these results, consider the numerical values of the calculated reflectivities $R(m)$. For the case without losses, the results of the $R(m)$ calculations for the three R_N values are given in the table. The table also shows the case for $R'(m)$ with rounding to 1% to illustrate the use of an FBG with rounded coefficients R'.

Table

Calculated dependence of FBG reflectivities R on the grating number m, with and without rounding

	R, without rounding			R, rounded to 1 %	
m	$R_N = R(0)=1$	$R_N = R(0)=0.1$	$R_N = R(0)=0.05$	$R_N = R(0)=1$	$R_N = R(0)=0.1$
18	0.0318	0.0242	0.01940	0.03	0.03
15	0.0339	0.0254	0.02018	0.03	0.03
14	0.0363	0.0268	0.02102	0.04	0.03
13	0.0391	0.0283	0.02193	0.04	0.03
12	0.0424	0.0299	0.02293	0.04	0.03
11	0.0462	0.0318	0.02402	0.05	0.03
10	0.0508	0.0339	0.02521	0.05	0.04
9	0.0564	0.0364	0.02653	0.06	0.04
8	0.0633	0.0392	0.02800	0.06	0.04
7	0.0722	0.0424	0.02964	0.07	0.05
6	0.0839	0.0462	0.03147	0.08	0.05
5	0.0999	0.0508	0.03355	0.10	0.06
4	0.1234	0.0564	0.03592	0.12	0.06
3	0.1605	0.0634	0.03865	0.16	0.07
2	0.2278	0.0722	0.04182	0.23	0.08
1	0.3820	0.0839	0.04555	0.38	0.10
0	1.0000	0.1000	0.05000	1.00	0.03

This study was performed within the framework of State Assignment for Basic Research (Code FSEG-2020-0024)

REFERENCES

1. **Jones J.D.C.,** 30 Years of the OFS conference: the origins and directions of our subject, Proceedings of SPIE – The International Society for Optical Engineering. 9157 (2014) 9157C2.

2. **Udd E., Spillman Jr W. B.** (Eds.), Fiber optic sensors: an introduction for engineers and scientists, John Wiley & Sons, Hoboken, New Jersey, USA, 2011.

3. **Measures R.M.,** Structural monitoring with fiber optic technology, Academic Press, Cambridge, Massachusetts, USA, 2001.

4. **Langhammer J., Eriksrud M., Berg C., Nakstad H.,** Fiber optic permanent seismic system for increased hydrocarbon recovery, In: Proceedings of the 11th International Congress of the Brazilian Geophysical Society, European Association of Geoscientists & Engineers, Salvador, Brasil, 24–28 Aug 2009, cp-195-00408.

5. **Plotnikov M.Y., Lavrov V.S., Dmitraschenko P.Y., et al.,** Thin cable fiber-optic hydrophone array for passive acoustic surveillance applications, IEEE Sensors Journal. 19 (9) (2019) 3376–3382.

6. **Akkaya O.C., Digonnet M.J.F., Kino G.S., Solgaard O.,** Time-division-multiplexed interferometric sensor arrays, Journal of Lightwave Technology. 31 (16) (2013) 2701–2708.

7. **Kersey A.D.,** Multiplexed interferometric fiber sensors, Proceedings of the 7th Optical Fiber Sensors Conference, December 2 – 6, 1990, The Institution of Radio and Electronics

Engineers, Australia, Sydney, New South Wales (1990) 313–319.

8. **Kostromitin A.O., Liokumovich L.B., Skliarov P.V., Kotov O.I.,** The fiber-optic interferometric schemes with multiplexed sensitive elements: an analysis of output optical power level, St. Petersburg Polytechnical State University Journal. Physics and Mathematics. 13 (2) (2020) 126–141.

9. **Liao Y., Austin E., Nash P.J., et al.,** Highly scalable amplified hybrid TDM/DWDM array architecture for interferometric fiber-optic sensor systems, Journal of Lightwave Technology. 31 (6) (2013) 882–888.

10. **Ren Z., Cui K., Zhu R., et al.,** Efficient and compact inline interferometric fiber sensor array based on fiber Bragg grating and rectangular-pulse binary phase modulation, IEEE Sensors Journal. 18 (23) (2018) 9556–9561.

11. **Yoshida M., Hirayama Y., Takahara A.,** Real-time displacement measurement system using phase-shifted optical pulse interferometry: Application to a seismic observation system, Japanese Journal of Applied Physics. 55 (2) (2016) 022701.

Received 30.09.2020, accepted 14.10.2020.

THE AUTHORS

LIOKUMOVICH Leonid B.
Peter the Great St. Petersburg Polytechnic University
29 Politechnicheskaya St., St. Petersburg, 195251, Russian Federation
leonid@spbstu.ru

KOSTROMITIN Aleksey O.
Concern CSRI "Elektropribor";
Peter the Great St. Petersburg Polytechnic University
30 Malaya Posadskaya St., St. Petersburg, 197046, Russian Federation
kostromitin.aleksei@yandex.ru

SKLIAROV Philip V.
Concern CSRI "Elektropribor";
Peter the Great St. Petersburg Polytechnic University
30 Malaya Posadskaya St., St. Petersburg, 197046, Russian Federation
sklyarov.fil@gmail.com

KOTOV Oleg I.
Peter the Great St. Petersburg Polytechnic University
29 Politechnicheskaya St., St. Petersburg, 195251, Russian Federation
kotov@rphf.spbstu.ru